Beam Physics Note
TRI-BN-21-15
August 20, 2021

CANREB High-Resolution Separator Commissioning Progress

Owen Lailey[1]

TRIUMF

Abstract: This document highlights commisioning results for the ARIEL CANREB High-Resolution Separator from May - August 2021. Emphasis is also put on explaining what scripts are used for continued commissioning work.

[1]University of Waterloo, 4A Mathematical Physics coop student from May - August 2021. Supervised by Suresh Saminathan and Marco Marchetto in the beam physics group. School email: oalailey@uwaterloo.ca

1 Introduction

The design of the High-Resolution Separator (HRS) is described in ref. [1]. The commissioning plan for the HRS is described in ref. [2]. All relevant scripts and files can be found on the TRCOMP01 server under user olailey (`/HRS/20210818_owen_all_work`). Alternatively, `jupyter.triumf.ca` has the TRCOMP01 file systems mounted so the files can be accessed there as well. Finally, the files will (eventually) get put on gitlab in the beamphys group folder (`https://gitlab.triumf.ca/beamphys`) in order to have an archive of HRS data.

2 HRS Layout

The CANREB HRS system is shown in figure 1. The separator consists of two identical ninety degree dipoles (AHRS:MB7A and AHRS:MB7B). A multipole (AHRS:MLTP7) is present in between the two dipoles to correct for high order aberrations. In the context of this report, the other relevant elements and diagnostics consist of XSLIT6, YSLIT6 and XEMIT6 at the entrance and XSLIT8, YSLIT8 and XEMIT8 at the exit of the HRS. A variety of other diagnostics, like the vertical emittance scanners, were unavailable for measurements at the time. Optical elements of interest are four quadrupoles, Q3-Q6, at the entrance of the HRS.
For commissioning, the beam transport path was ALTIS-ALTS-ALTW-AHRS (see figure 2).

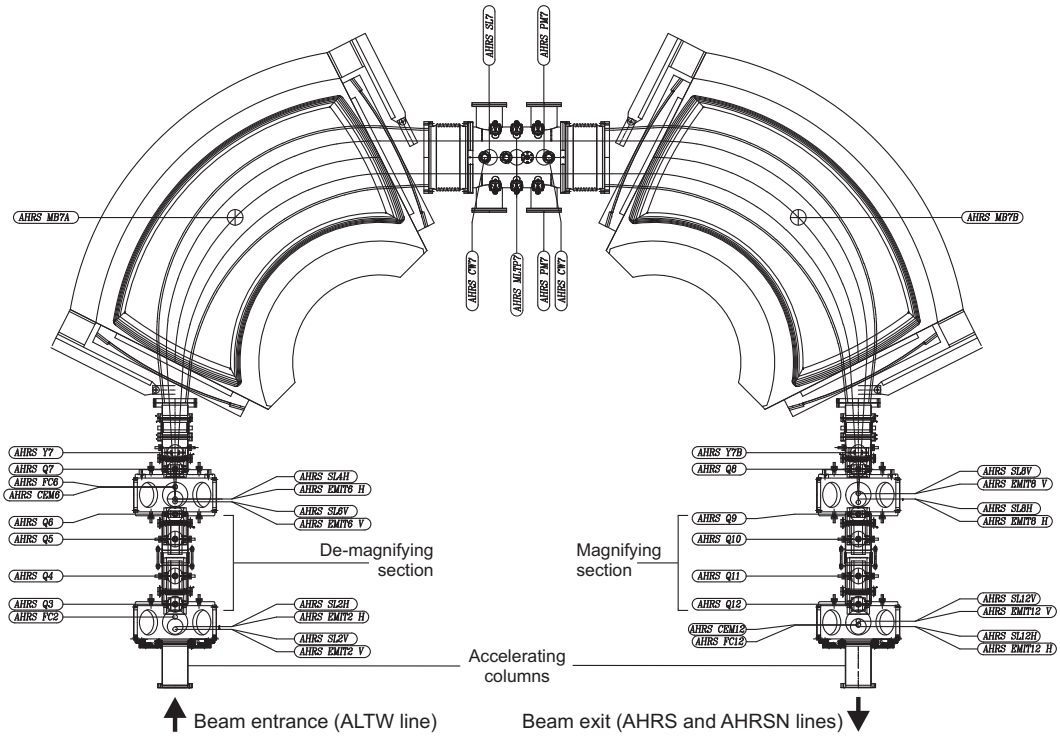

Figure 1: Layout of the CANREB HRS beamline.

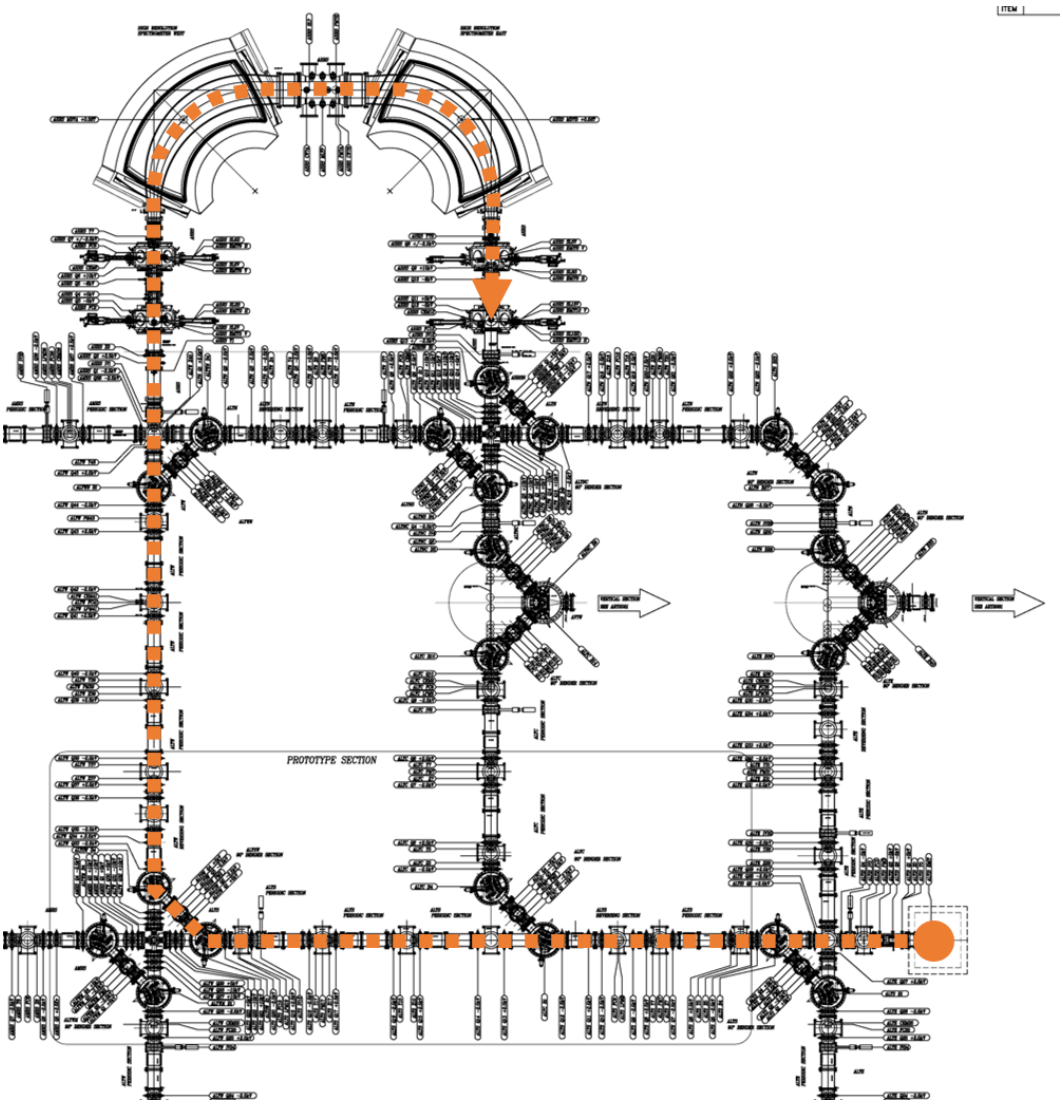

Figure 2: Beam path used for commissioning from the ALTIS up to and through the HRS at the ARIEL B-2 level (ALTIS-ALTS-ALTW-AHRS).

3 10k RP Emittance Scans

The HRS is designed to achieve a mass resolving power (RP) of 20,000 for a transmitted, transverse beam emittance (4*RMS) of 3 μm [1]. Prior to May 2021, commissioning work at 5k and 10k RP was ongoing (refer to [3] for different RP tune details). All measurements in this report were using the 10k RP tune. The main point of investigation at 10k RP is the emittance growth through the HRS. Two possible causes of emittance growth include (note there are many others): transverse plane coupling and energy spread. It is a priority to figure out what is the cause of the emittance growth and how to correct it.
Figure 3 shows the calculated beam envelope through the HRS for a 30 keV beam with a given transverse 4RMS emittance of 3 μm. The calculated 2RMS beam size in the horizontal plane (x) at the location of XSLIT6 and XSLIT8 is 0.2 mm for 5k RP. For 10k RP, the 2RMS size is 0.1 mm at these locations.
In this report, all emittance measurements at XEMIT6 and XEMIT8 are analyzed and plotted via Rick Baartman's Matlab scripts (refer to `http://lin12.triumf.ca/emittance/emitmat/`). The scripts contain processing tools to remove noise and calculate various beam properties.
One important note about the emittance plots is that the angles on the y-axis are calculated differently then is expected based on the voltage range used in the measurement. Referring to `emitmat.m` and `processdata.m`, theta offset and conversion factors are calculated using plate length, plate gap and voltage offsets given in the scan file. The voltage range is assumed to be symmetric and then it factors in an offset value given in the scan file for an asymmetric range. I think there might be some confusion at this step since the theta offset value given in the scan file is actually the starting voltage value in the scan (i.e not the value the range should be centered around). For example, a scan in the voltage range 100V to 900V will be mostly centered in angle in the Matlab emittance plot with an angle offset corresponding to the 100V starting value (see figure 6). Other scripts, that only care about the voltage range used, calculate the angle with $angleMrad = plateBiasV * 28/(4 * 2 * beamEnergyKV)$. Following the 100V to 900V scan example, this would correspond to an angle range of about 12 to 105mrad (i.e not centered around zero like the Matlab scripts).

3.1 Potassium Ion Source

A Potassium ion source was used for all measurement up until July 6th. At 10k RP, we took XEMIT6 and XEMIT8 scans for beam energy of 30, 40 and 50 keV (see figure 4). A major point of investigation is the emittance growth that is seen between XEMIT6 and XEMIT8 (see table 1). At higher energies, the measured XEMIT8 emittance decreases as expected. However, the *normalized* 4RMS emittance at XEMIT8 also decreases significantly. To determine if this is an energy spread effect, Rick analyzed the results as followed: if there is a component that comes from energy spread, then this will show up as an addition to the rms (waist) size, added in quadrature. So, squaring the XEMIT8 waist value, subtracting the square of the

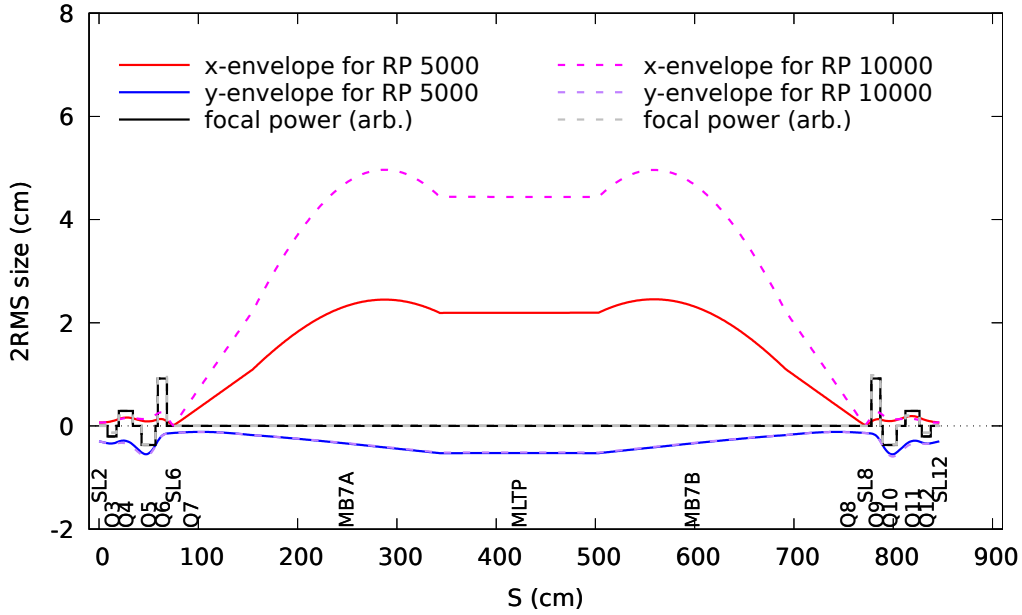

Figure 3: Calculated beam envelope through the HRS for a given emittance of 3 μm by using the code TRANSOPTR. 2RMS beam sizes are plotted for both 5k and 10k resolving power.

XEMIT6 value and square rooting gives contributions 0.164, 0.127, and 0.120mm for 30, 40, 50kV cases respectively. The contribution from energy spread would be scaled as energy dispersion times dE/E and thus scales as $1/E$ for fixed dE. Multiplying by 30, 40, 50 kV gives 4.9, 5.1 and 6.0. These values are pretty constant when taking into account expected error will be about 1. Since we know that the energy dispersion is 2400mm, we can be even more quantitative to get the 2rms energy spread. Simply divide 0.164, 0.127, and 0.120mm by 2400 and multiply by energy in volts. This gives a 2rms energy spread of 2.05, 2.1 and 2.5 eV for beam energy of 30, 40 and 50kV respectively. These calculations indicate that since the energy spread is independent of beam energy, it can be something added to the system (i.e like a ripple in the ground). Work is ongoing to re-ground the HRS and see if this solves the emittance growth.

3.2 Rubidium Ion Source

In mid-July, the source was switched from Potassium to Rubidium. A heavier mass and the two peaks for 85Rb and 87Rb are helpful for characterizing the system during commissioning (fig:5). We took 10k RP XEMIT6 and XEMIT8 scans at 30keV beam energy for 85Rb as shown in figure 6. The emittance growth is still evident as the 4rms emittance changes from 3.01 μm to 5.2 μm between XEMIT6 and XEMIT8. Despite the emittance growth, the beam at XEMIT8 is nicely rounded and has no aberrations even with the multipole turned off.

	XEmit6			
Beam Energy (keV)	4rms emit (um)	norm 4rms emit (um)	2rms waist (mm)	2rms th waist (mrad)
30	2.91	0.003745	0.115121	20.31289
40	2.35	0.003495	0.100679	19.127023
50	2.15	0.003559	0.096092	18.5258
	XEmit8			
Beam Energy (keV)	4rms emit (um)	norm 4rms emit (um)	2rms waist (mm)	2rms th waist (mrad)
30	5.13	0.006593	0.200455	25.587684
40	3.43	0.005085	0.162447	21.057040
50	3.24	0.005374	0.154027	20.839264

Table 1: Comparison of XEMIT6 and XEMIT8 4RMS emittance values for different beam energy values at 10k RP. The top rows are from XEMIT6 and the bottom rows are from XEMIT8. The second column gives the measured 4RMS emittance values. The third column gives the normalized 4RMS emittance values. The fourth and fifth columns give the 2RMS waist values.

3.3 Degaussing and Ramping HRS Dipoles

Proper degaussing and ramping of the two HRS dipoles is necessary for optimizing the field flatness of the dipoles (described in section 9 of ref. [1]). Spencer Kiy wrote a document on the proper HRS ramping procedure from when the dipoles were installed in the magnet test stand area [4]. It is important to carefully degauss and ramp the HRS dipoles according to a tested procedure as a significantly varying field reduces beam quality through the HRS. Unfortunately, the dipole polarity switches were not yet made controllable and thus we were unable to try any degaussing routines (general degaussing HLA here: `https://beta.hla.triumf.ca/degaussing/`). However, progress was made in developing and testing a ramping HLA for the HRS.

Spencer helped with all of the web development for an HRS specific ramping HLA deployed here: `https://beta.hla.triumf.ca/degaussing/HRS-ramp/`. As described in the ramping procedure document, dipole ramping involves ramping the current past the desired setpoint to an overshoot value and then ramping back down to the desired setpoint. Figure 7 is a plot based on the data from the ramping document and is used for calculating the overshoot value to use based on the desired setpoint. The desired setpoint is calculated using the excel file: `HRS_calculate_dipole_field.xlsm`.

For the ramping HLA, some work was put into trying to properly calibrate the CURROC values so that the user knows what the ramp rate is (A/s) for a particular CURROC setting. The app may still yet require some further calibration so the dipoles ramp at exactly the speed that is set. This will be more important when trying several different ramps with different ramping speeds and seeing the effect on the beam through the HRS.

One interesting ramping test we did involved ramping the dipoles very slowly (both

up and down) and then very fast (both up and down) and comparing what the beam looked like at the exit of the HRS. The first ramp we did was starting MB7A at 2.28A and MB7B at 2.43A and ramping to 85A each for CURROC set to 0.1. Note that this ramp is slightly abnormal as a normal ramp would start at 0A and go to calculated overshoot values. Next, we ramped down to about 65.3A for both dipoles (desired setpoint for 85Rb) with CURROC set to 0.1. Based on the current app calibration, this is a ramp rate of about 0.013 A/s. However, note that during testing Spencer mentioned that there is a minimum ramp rate of the power supplies at about 0.03 A/s which currently corresponds to CURROC set at 0.23. Regardless, we did this slow ramp up/slow ramp down and obtained the XEMIT8 scan in figure 6.

As a type of worst case scenario test, we then ramped the dipoles following the same procedure except with CURROC set to 10 (about 1.33 A/s). Figure 8 shows the XEMIT8 scan following the fast ramp test. The beam is still nicely rounded and has no aberrations. However, the 4RMS emittance has grown from 5.2 μm to 5.68 μm. This is a good example of how a poor ramp can effect the beam through the HRS. Further testing should be done with different ramps (i.e slow up/fast down) to optimize the field flatness and to see if the emittance at XEMIT8 can be improved further with an optimal field. Additionally, a full procedure of degaussing the magnets and ramping the dipoles should be conducted as soon as the polarity switches are controllable and the degaussing HLA is tested and workable with the HRS dipoles.

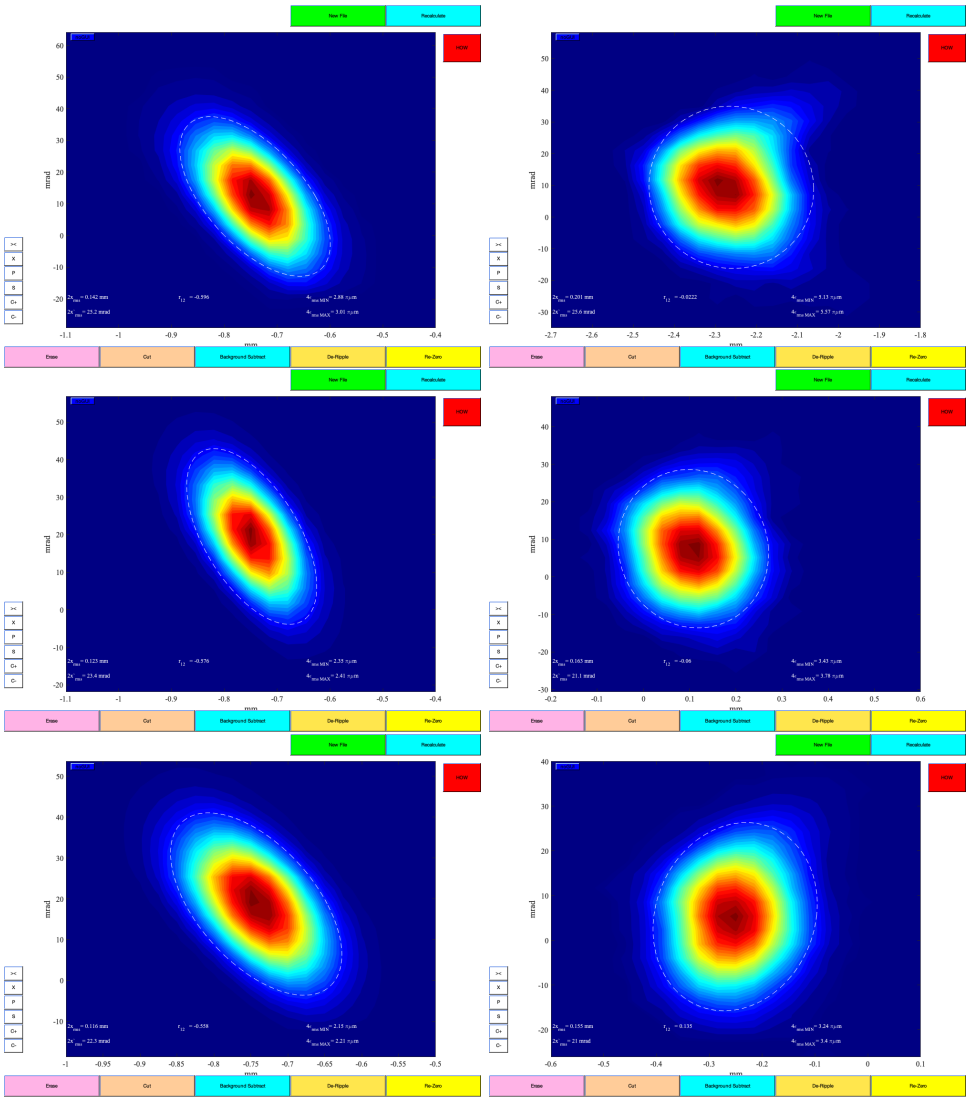

Figure 4: 10k RP emittance scans. XEMIT6 is the left column and XEMIT8 is the right column. From top to bottom, the rows are 30, 40 and 50 keV beam energy. Note that position and angle ranges varied from scan to scan at the different energies.

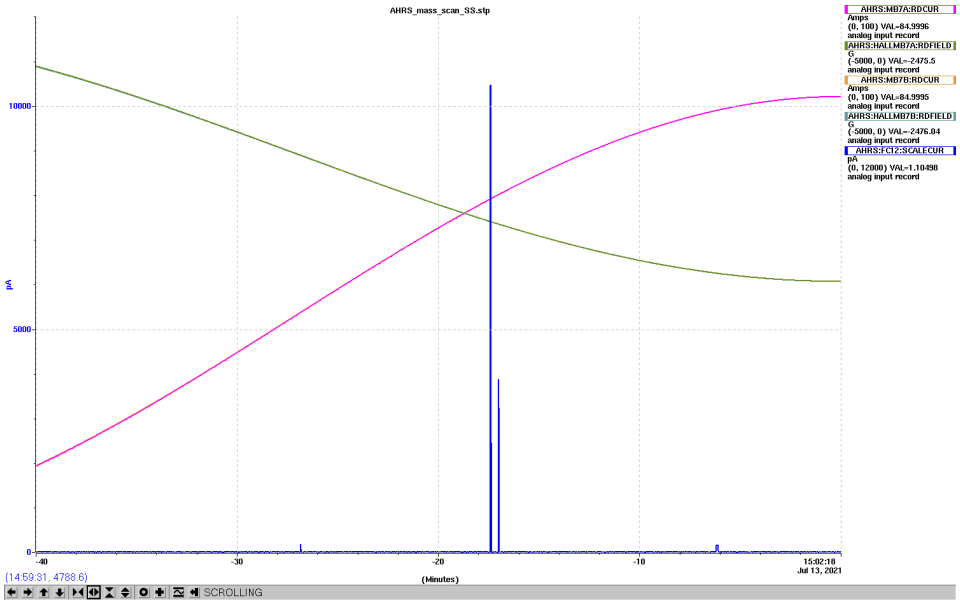

Figure 5: Mass scan through the HRS dipoles with Rubidium source. Small peaks at 39K and 133Cs and larger peaks at 85Rb and 87Rb as expected.

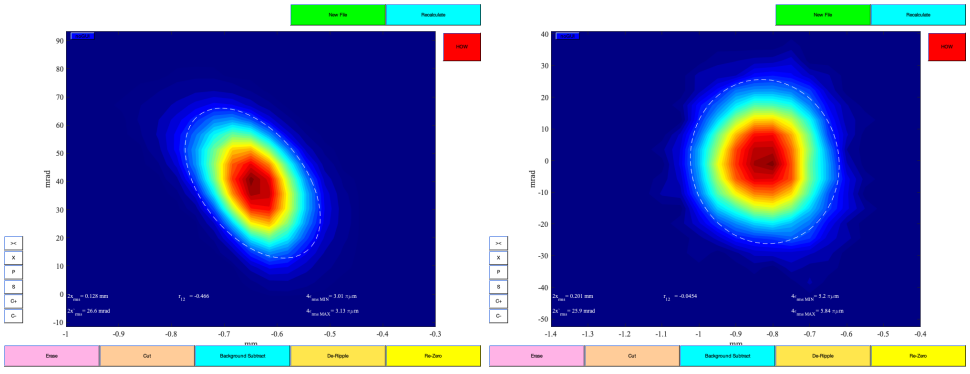

Figure 6: 10k RP XEMIT6 and XEMIT8 scans at 30keV beam energy for 85Rb through the HRS. Emittance growth from 3.01 μm to 5.2 μm between XEMIT6 and XEMIT8. Notably, the beam at XEMIT8 is nicely rounded and has no aberrations even with the multipole turned off.

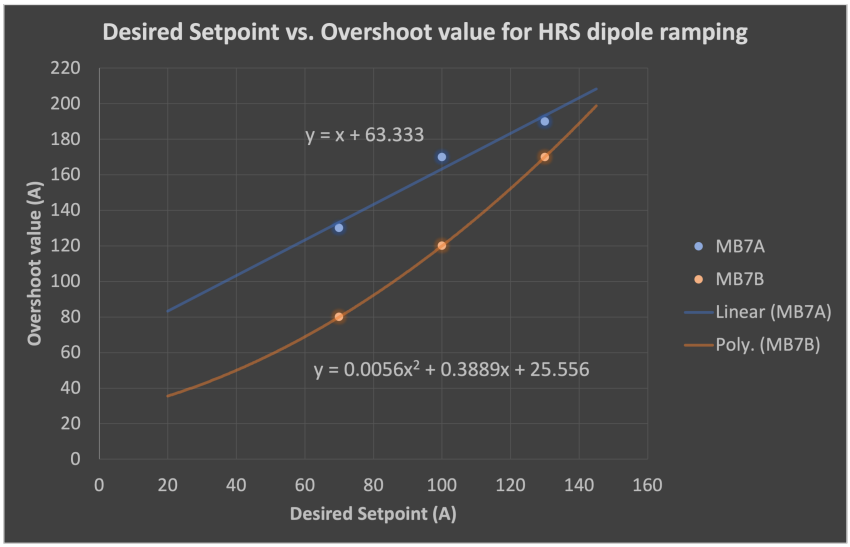

Figure 7: Equations for calculating the ramping overshoot value based on the desired setpoint for each of the HRS dipoles. Data points are from the ramping procedure document [4]. The last data point from the document is excluded as it is near the power supply limits and less trustworthy. MB7A data was fit with a linear trendline. MB7B data was fit with a quadratic trendline as a linear trendline would predict overshoot values that are less than the desired setpoint in the low current range.

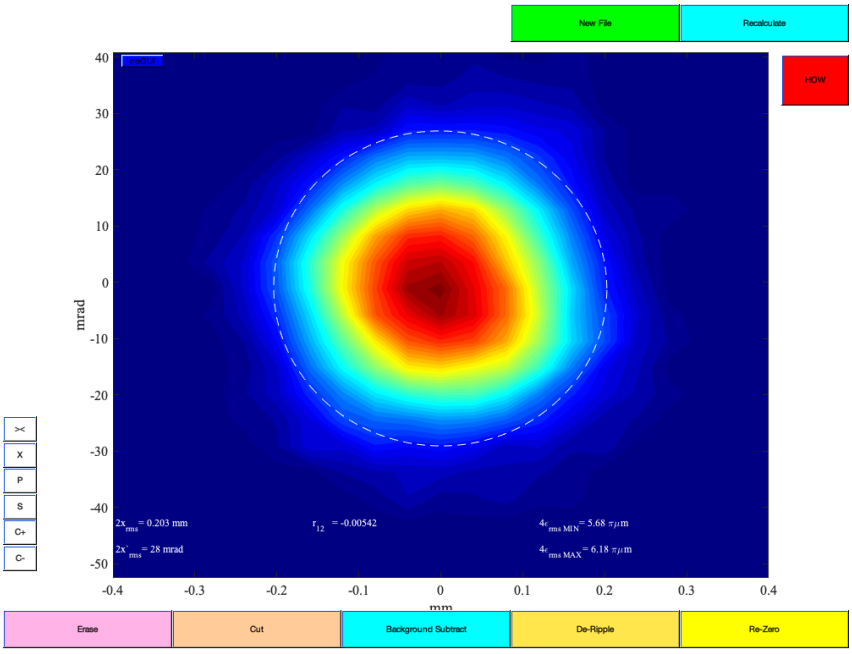

Figure 8: 10k RP XEMIT8 scan for 85Rb through the HRS. Notably, the 4RMS emittance has grown to 5.68 μm after testing a very fast ramping procedure. The fast ramp would impact the field flatness and serve as a sort of worst case scenario to see how the beam is effected through the HRS.

4 Tomography

Tomography work was done at the HRS entrance using XSLIT6 and YSLIT6. Tomography is a useful tool for comparing with results from the emittance scanners. Also, since the vertical emittance scanners are not yet controllable, tomography reconstruction in the vertical plane can provide some information on the vertical emittance. Unfortunately, XSLIT12 and YSLIT12 at the HRS exit were not yet controllable and thus we could not do any tomography reconstruction at the XEMIT8 location. This would be very helpful to have tomography comparison at this location to verify the emittance growth that is seen and to again, have some information on the vertical emittance.
Many beam physics notes have been written in the last few years on maximum entropy tomography reconstruction at TRIUMF (using various PMs). For work from TRIUMF beam physicists, see [5, 6, 7, 8]. For work from coop students, see [9, 10, 11, 12, 13]. Most of the scripts used for analysis are built off of the work in these papers. Refer to these notes for a basic understanding of how maximum entropy tomography works as well.

4.1 AHRS:XSLIT6 and YSLIT6

At the HRS entrance, there are four quadrupoles upstream of XSLIT6 and YSLIT6. `TRANSOPTR` simulations are used to determine which quadrupole should be scanned for tomography reconstruction. The `sy.f` file in the folder entitled `HRS_optr_tmat_and_rms_saving` simulates beam transport through the HRS. This file was modified to loop over a voltage array and automatically save the horizontal (X) and vertical (Y) 2RMS values at the entrance slit location (saved to `fort.7`). Additionally, the transfer matrices are automatically saved. This method of looping within the `sy.f` file requires the use of the `cic` function so that the initial conditions are being reset to the same values for each loop through the optical elements. The user must update which quadrupole is being scanned via the `qscan` variable and the folder location for saving. The other quadrupoles should be set via `data.dat` as usual. The python script `plot_beamsize_from_transoptr.py` is used to verify whether the quadrupole scan $2Xrms^2$ and $2Yrms^2$ values produce an adequate parabola for tomography reconstruction. Scanning Q4 with Q3 at 1.5kV and Q5, Q6 off, produced the desired parabola in both planes (see fig:9). The solid lines represent the `TRANSOPTR` values and the points are the measured values for XSLIT6 and YSLIT6 (measured profile processing done with `SLIT_PM_LPM_profiler_v3.py` and plotted via `integral_and_rms.py`). There is decent agreement between simulation and measurement.
The script, `SLIT_for_tomo.py`, is used to write the input file for MENT. This python script is where the user adjusts the number of profiles that MENT will use in the reconstruction. The next step is setting the input tomography variables in the `in` file and running MENT. In my experience, there is a lot of trial and error adjusting the variables: `Max Iterations, Interpolate N, and Smooth Factor`, in

order for the algorithm to converge to a solution. Typically, for phase space, I try 100 iterations, interpolate number set 300-500 and the smooth factor from 3-9. Adjusting the number of profiles and these three variables greatly affects convergence and how well the profiles are reconstructed. The python script, `general_contour_plot`, is used to plot the reconstructed beam in the transverse phase space planes (see fig:10). Overall, the reconstruction seems very good. The slight distortions/cusps in the horizontal beam are artefacts of poor data collection of the profiles. This is just a control issue and should be resolvable.

The script, `compare_input_output.py`, is used to compare the input (measured) profiles versus the output (reconstructed) profiles as seen in figure 11. These plots are some of the most useful for checking whether the tomography reconstruction is trustworthy. The reconstructed profiles should closely match the input profiles for convincing phase space plots and emittance calculations. In this case, the reconstructed profiles match very well other then the unfortunate ridges in the profiles that are from the data collection and not the actual beam. The profile plots are also helpful for showing how many profiles were used in the reconstruction. Many horizontal profiles were used for the reconstruction in this plane and thus the data seems very convincing. However, only three profiles were used in the vertical reconstruction. MENT excels at tomography reconstruction with a minimal number of profiles. Although, for our purposes, it is better to have a couple more profiles to ensure that we are not omitting information from alternate projections. I tried including other profiles in the reconstruction but noticed odd streaking effects that tend to be an artefact of some MENT reconstructions (i.e not real). Therefore, the vertical reconstruction provides some helpful information of the beam while we are lacking the vertical emittance scanners but it is highly recommended to repeat some quadrupole scans at the HRS entrance for further testing.

In terms of the emittance, the 4rms calculations based on the tomography reconstruction are relatively close to the expected input beam transverse emittance of $3\,\mu$m. Figure 12 shows the comparison between the tomography reconstruction and the XEMIT8 measurement. Since tomography reconstructs the beam further upstream (depending on where the `sy.f` file starts), we have to either transport the measurement upstream to the reconstruction location or the reconstruction downstream to the emittance scanner. Rick's Matlab emittance scripts allow for this via the `transform.m` file. I obtained the transfer matrix from `TRANSOPTR` based on the operational quadrupole settings used to take the measurement. Invert the matrix and input this in the transform function to transport the measurement back to the same location as the tomography reconstruction (as seen in fig:12). Qualitatively, there is good agreement. Table 2 shows beam size and emittance calculations for a quantitative comparison. Overall, the agreement is reasonable and further validates both measurement methods.

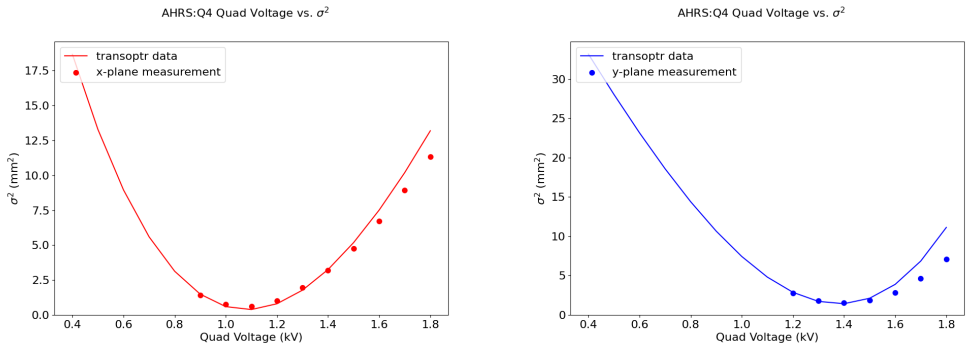

Figure 9: 2rms beamsize values squared versus AHRS:Q4 voltage. Q3 is set at 1.5kV and Q5, Q6 turned off. The solid line represents `TRANSOPTR` values and the points represent measurements from XSLIT6 (left) and YSLIT6 (right). Full parabolas are visible in both planes which is required for tomography reconstruction. There is decent agreement between simulation and measurement as well. Plots produced via `integral_and_rms.py`.

	2Xrms	2X'rms	r12	4ϵrms
XEMIT8	0.81 mm	4.20 mrad	-0.389	3.15 μm
Tomo Reconstruction	0.82 mm	4.36 mrad	-0.341	3.36 μm

Table 2: Comparison of beam properties between an XEMIT8 measurement and tomography reconstruction as seen in figure 12. Overall, there is relatively good agreement. This comparison helps validate both the emittance scanner and the tomography reconstruction method due to the close agreement.

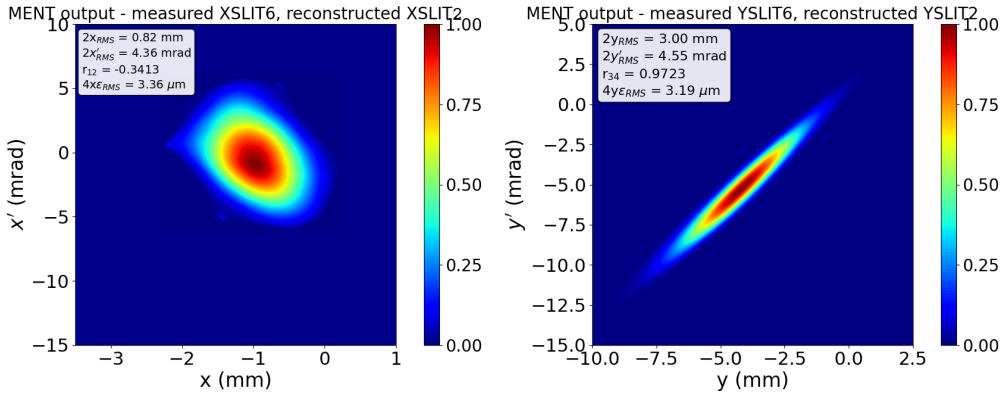

Figure 10: Tomography reconstruction phase space plots in the horizontal (left) and vertical (right) planes. Profiles measured with XSLIT6 and YSLIT6 and reconstructed upstream at SLIT2 location. Overall, reconstruction seems very good. Slight distortions/cusps in horizontal beam are artefacts of poor data collection of the profiles (see the ridges/steps in fig:11 profiles). The vertical reconstruction is quite spectacular but an important disclaimer is that this reconstruction only used 3 profiles. MENT is excellent at reconstructing with minimal profiles but for more confidence in the reconstruction matching measurements, more profiles should be used. It is recommended that more scans are done at this location to try and use more profiles in the vertical reconstruction. However, despite only using 3 profiles, this vertical reconstruction still gives helpful information about the vertical phase space since the vertical emittance scanners are not yet controllable. Both reconstruction were done with 100 iterations, interpolate number of 500 and a smooth factor of 3 in the MENT input file.

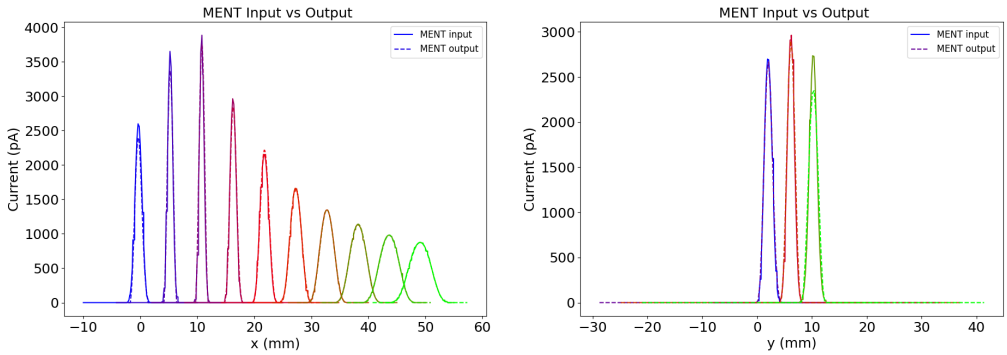

Figure 11: Comparison of the input (measured) profiles with the output (reconstructed) profiles. In general, the profiles match very well for both x (left) and y (right) planes. Poor data collection of the profiles results in ridges that mostly get smoothed out in the reconstruction. These ridges are not a real aspect of the beam and should be fixed for better reconstruction. MENT is excellent at reconstructing with minimal profiles but for improving confidence in the reconstruction matching reality, more profiles should be used. It is recommended that more scans are done at this location to try and use more profiles in the vertical reconstruction. Despite only using 3 profiles, this vertical reconstruction does still give helpful information for vertical phase space since the vertical emittance scanners are not yet controllable.

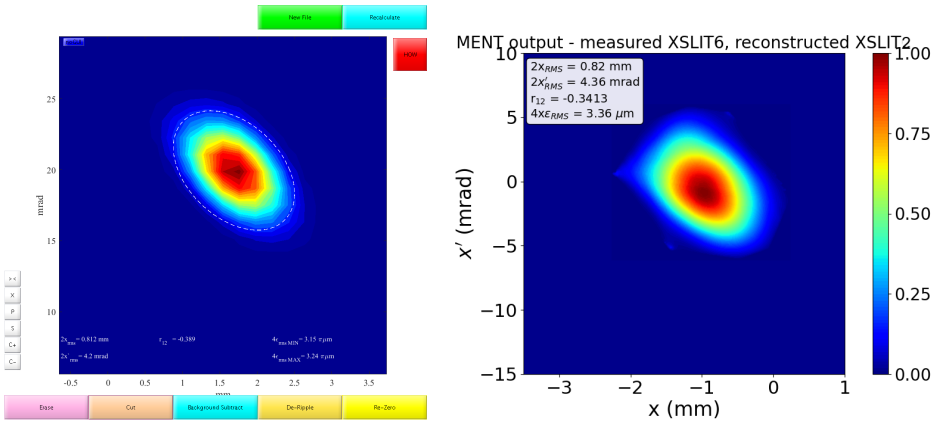

Figure 12: 30 keV 39K beam at 10k RP tune. XEMIT8 measurement (left) transported to the XSLIT2 location to compare with tomography reconstruction (right). Note: the vertical and horizontal scales on the plots are very similar but not identical. For a more quantitative comparison, see table 2.

5 Multipole

The HRS multipole is used to correct higher order aberrations. The design of the multipole is described in ref. [14]. Figure 13 shows the drawing of the multipole consisting of 23 electrode pairs.

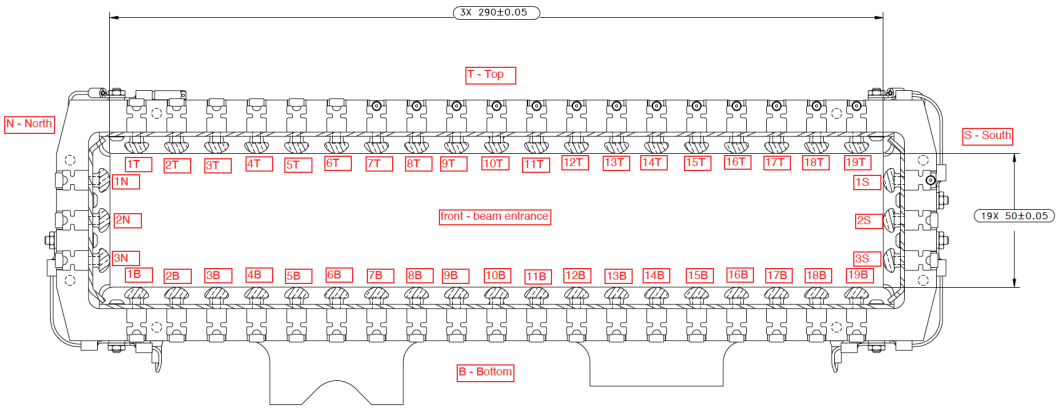

Figure 13: Drawing of the HRS multipole. Labels correspond to naming convention in EPICS. The multipole wire is spatially aligned with pole 10 in the drawing. For initial testing of the multipole, poles 9, 10 and 11 were turned on to see the effect on the beam.

5.1 Measurements

As a part of the commissioning process, we initially tested inserting the multipole wire to see the effect on the beam at XEMIT8 (fig:14). The wire is spatially aligned with pole 10 of the multipole and creates a cut in position at the multipole location that maps to a cut in angle at the XEMIT8 location.
Next, we tested the multipole by turning on individual poles and seeing the effect on the beam at XEMIT8. Turning on the central pole (pole 10) to 200V resulted in a splitting/shearing effect that exceeded the position scanning range in the XEMIT8 measurement (1.1mm). In other words, 200V on pole 10 was much larger than necessary and sent the beam outside the scan window. Turning on pole 10 to -5V showed that just a 5V magnitude is large enough for a significant splitting effect on the beam (fig:15).
We tested two off-centered poles to have measurements for pole 9, 10 and 11 at $\pm 5V$ each (fig:16). Qualitatively, the level of splitting/shearing seems to match what is expected based on spatial location of the pole and also the sign of the applied potential. It is recommended that each pole is tested in a similar fashion to verify they are all individually working as expected.

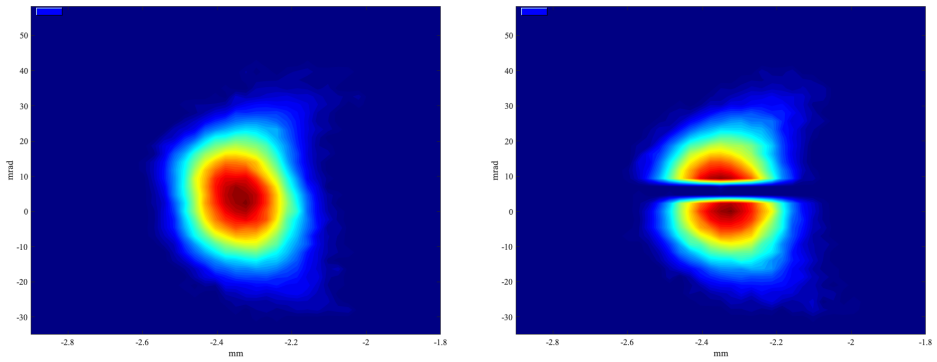

Figure 14: 30keV 39K beam with 10k RP tune, high resolution (40x40 points) XEMIT8 scans. The right image is when the multipole wire is inserted. We observe how the cut in position at the multipole is converted into a cut in angle at XEMIT8 location.

5.2 ZGOUBI Simulations

After taking these measurements, I worked on ZGOUBI simulations for the purpose of 1) Confirming that the Multipole was having the expected effect on the beam and 2) Developing a working model of the HRS and Multipole in ZGOUBI such that we can optimize the multipole configuration to correct for aberrations (see section 5.3).
A significant amount of ZGOUBI simulation work was done several years ago by Thomas Planche and coop student Dan Sehayek for the HRS. Thomas has two fairly comprehensive ZGOUBI tutorials for the HRS which are helpful to go through first [15]. One small word of warning is that I have found one typo in some of the files that will greatly effect how much voltage the multipole puts on the poles (further discussed below).
The ZGOUBI input file `30kV_U1+_multiparticle.in` is used for doing multiparticle simulations through the HRS while turning on poles of the multipole. This input file is based off of Thomas' `multiparticle.in` file. The main differences between the two files are:

- Brho value changed from 543.687 $[Kg \cdot cm]$ to 384.445 $[Kg \cdot cm]$ (divide by $\sqrt{2}$) to go from 60keV beam to 30keV beam in 'OBJET' element. This change was made since we mostly use a 30keV beam for commissioning.
- As a result of changing Brho, the magnetic field scaling factors in the 'TOSCA' elements need to change by the same factor. i.e from 1.0318 to 0.729593 in this case.
- Initial particle distribution scaling factors were changed in the 'OBJET' element to better match measurements taken under 10 RP tune (`2.5 0.4 2.0 0.25 1. 1.`). The adjusted scaling factors change beam size in position and angle for horizontal and vertical planes but keep 3 μm input transverse emittance.

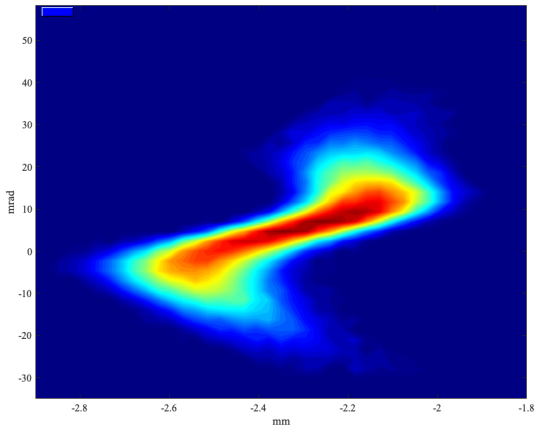

Figure 15: High resolution (40x40 points) XEMIT8 scan with pole 10 of the multipole turned on to -5V. 30keV 39K beam with 10k RP tune through the HRS.

- Lastly, the important typo was the mass given in the 'PARTICUL' element. Originally, it was 22172.3 MeV/c^2 which is about a factor of 10 off of the correct mass of $221697 MeV/c^2$ for 238U ($931.5 MeV/c^2 * 238u$). In simulations, this affects the potential the multipole puts on the poles. For example, the multipole would put around -50V on a pole (due to the typo) where in reality it would only need about -5V on that pole for the same effect (see figure 17). This mistake shows up more prominently in Dan's work where he is trying to optimize the multipole configuration but is applying voltages that are too large then needed in reality.

The python script, `Multipole.py`, is used to run ZGOUBI with specific poles of the multipole turned on. The script reads individual field maps for every single pole at a 1V potential. Then, the contributions from each pole are added together and written to a field map that ZGOUBI uses between the two dipoles in `30kV_U1+_multiparticle.in`.
The script and the modified input file allow for ZGOUBI simulations that can compare to previous measurements (see figure 18). These simulations show great quantitative comparison to measurements. Applying the same potential in the simulations shows the same levels of splitting/shearing as in measurements. This satisfies the first goal of showing that the multipole is working as expected for commissioning (for the three poles tested at least). It also verifies that the model in ZGOUBI is accurate enough to attempt to use it for optimizing the multipole configuration when given emittance data with aberrations. Note that in figure 18 the results are artificially centered to lie on top of each other since measurements are not typically centered very well.
A few more notes about the simulation beam properties: the initial distribution has 3 μm emittance in both horizontal and vertical planes. It is also a hard edge beam which helps explain why the simulations don't exactly match the contour plots (i.e

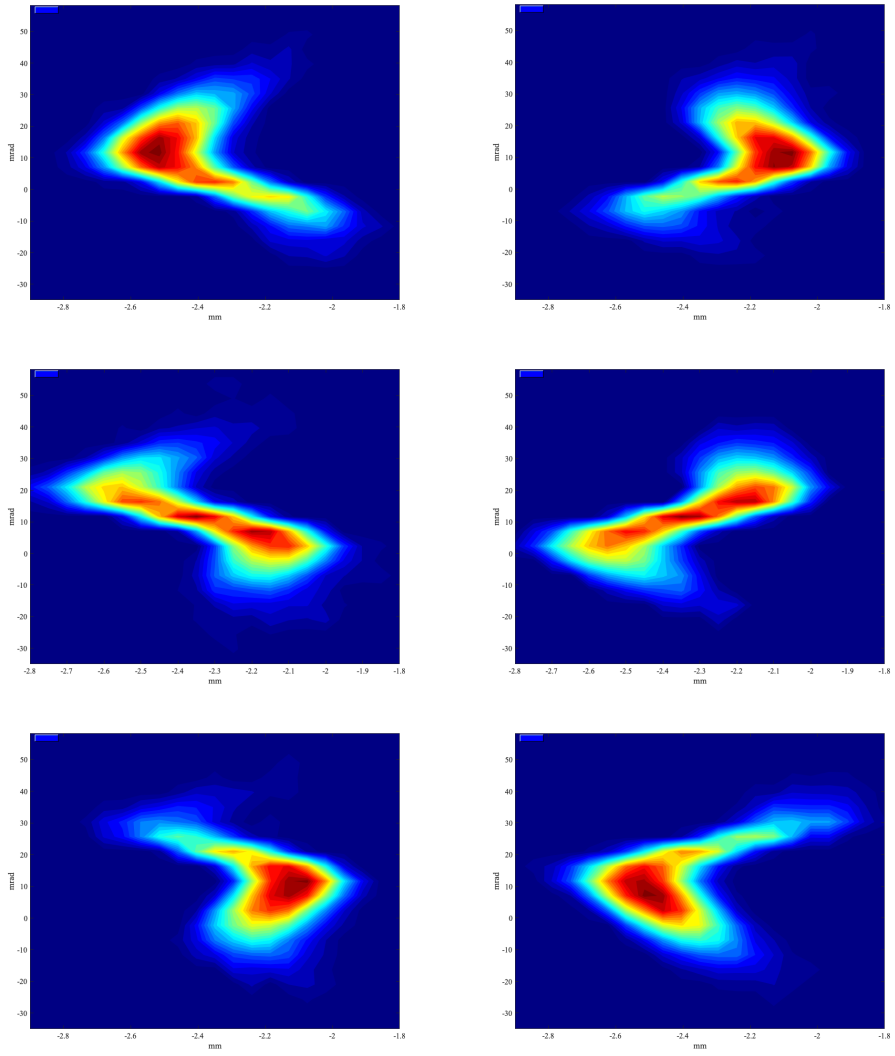

Figure 16: 30keV 39K beam with 10k RP tune XEMIT8 scans with one pole of the multipole turned on. From top to bottom, the rows are pole 9, 10 and 11. The left column is the pole at +5V and the right column is -5V.

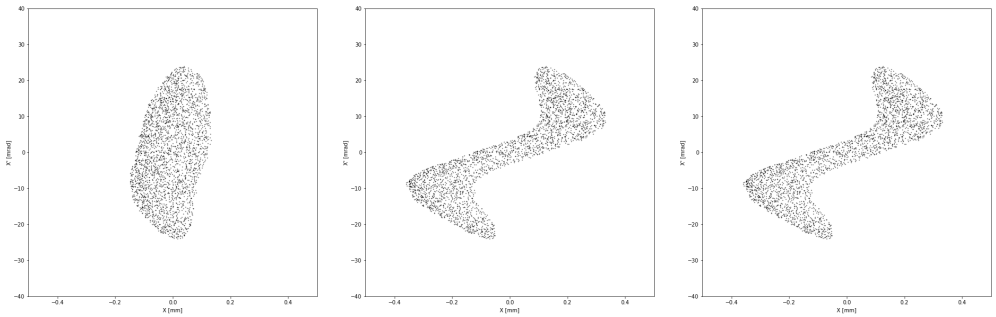

Figure 17: Horizontal phase space simulations in ZGOUBI through the HRS. From left to right: 1. wrong mass of 22172.3 MeV/c^2 with -5V on pole 10, 2. wrong mass of 22172.3MeV/c^2 with -50V on pole 10, 3. correct mass of 221697MeV/c^2 with -5V on pole 10. Simulations seem to qualitatively match measurements (see figure 15) for the second and third plots above. This also shows how, qualitatively, the same result is produced when the mass is off by a factor of 10 but the pole magnitude is increased by a factor of 10.

beam is more Gaussian in reality). Furthermore, the simulations shown in figure 18 were done with no energy spread. Different levels of energy spread can be added by using `change_Espread.py` and using the file it generates as the input beam distribution in the ZGOUBI input file. Simulations were done with energy spread and they show the distribution 'fuzzing' out to slightly improve the match with measurements (fig:19). This could help explain that an energy spread issue is the reason we are seeing emittance growth through the HRS.
One last important note has to do with the orientation in EPICS (i.e measurements) compared to the orientation in ZGOUBI and python. First, in python, indexing starts with 0 and so the 23 poles are indexed from 0 up to 22. This means index 11 in python is pole 10 of the multipole. Also, the orientation in simulations is flipped compared to measurements. This means that 'pole 11' in simulations is pole 9 in reality. Combining these two factors, we have that index 10, 11, 12 in python simulations corresponds to pole 11, 10, 9 in EPICS/measurements (see table 3). I recommend that more measurements are done (i.e individually turn on all the poles) to confirm that this simulation to measurement mapping is correct. The current mapping is only based on how well simulations match measurements for poles 9, 10, and 11. Testing all the poles will also verify that all the polarities are correct. The orientation has further implications in the next section when trying to optimize the multipole configuration for fixing aberrations.

5.3 Optimizing Multipole Configuration

As mentioned in the last section, Dan Sehayek worked a lot with ZGOUBI simulations and developed an algorithm that would read in an emittance measurement

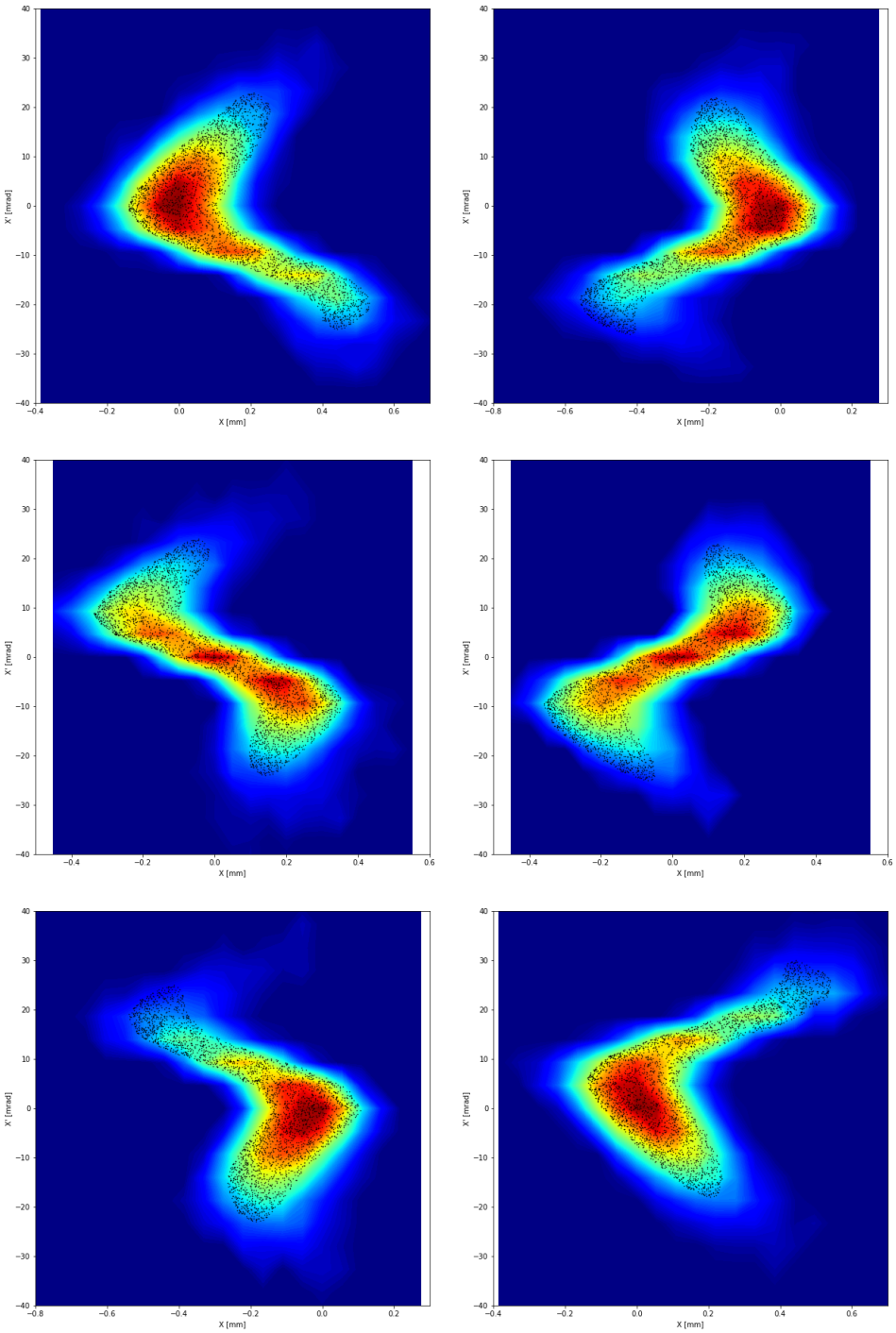

Figure 18: 10k RP XEMIT8 scans (the contour plots) with one pole of the multipole turned on. The scatter point distributions are simulations in ZGOUBI plotted on top of the measured data. From top to bottom, the rows are pole 9, 10 and 11. The left column is the pole at +5V and the right column is -5V. Measurements and simulations are artificially centered to lie on top of one another.

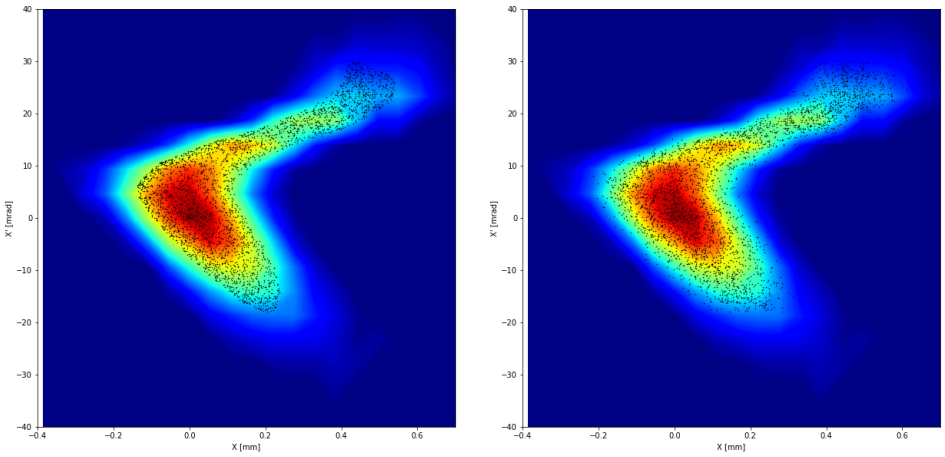

Figure 19: 10k RP XEMIT8 scans (the contour plots) with pole 11 of the multipole at -5V. The left plot is the ZGOUBI simulation with no energy spread. The right plot is the ZGOUBI simulations with 2eV energy spread. Observe how including some energy spread improves the matching between the simulation and measurement. This could help explain why we are seeing emittance growth through the HRS at the time of writing.

in horizontal phase space and return the multipole configuration that is needed to correct the aberrations in the measurement. Refer to [16, 17] for the algorithm details. A gitlab repository for the HLA code is here: `https://gitlab.triumf.ca/hla/atom` and is deployed here: `https://devel.hla.triumf.ca/atom`. His original files can be found here: `https://jupyter.triumf.ca/user/olailey/tree/home/dsehayek` (where you would be the user and not olailey) and also via the TRCOMP01 server. Note that minimal work has been done on changing the actual HLA from when Dan worked on it. The priority was on fixing the actual scripts (i.e the algorithm) to agree with measurements before worrying about deploying a half-working app.

Since all of this work took place several years before the HRS was even at the commissioning stage, all of Dan's work was using simulated data. This meant that the code could never be tested on real data to see if it actually works. Initial tests using the HLA with real data gave configurations that did not make any physical sense. The optimized configuration would have multiple different poles at $\pm 1000V$. This contradicts measurements in section 5.1 where $\pm 5V$ can be enough to significantly move the beam. In fact, even with simulated data it can be seen on the last page in [17] that multiple poles are at suspiciously large potentials.

The first error that was affecting the optimizer has to do with the mass error in the ZGOUBI input file that was mentioned in section 5.2. The algorithm used to optimize the configuration requires a table of values from ZGOUBI that represent the change in a particles position at a certain angle for a certain pole at 1V. This table is generated using `MultipoleTable.py` which runs ZGOUBI in a loop over different

poles. Due to the error in the ZGOUBI input file, this table was completely wrong and was contributing to the algorithm putting large potentials on the poles.
Another error that was affecting the optimizer has to do with how the code was calculating the reference center of the emittance data. In general terms, the code figures out the centroid all along the beam, which may look like an S or C shape due to aberrations. The code calculates what the central position of the beam is (i.e some reference vertical line). Then, the optimizer wants to apply potentials on the poles to make that odd S or C shape look like a straight vertical line (i.e no aberrations) by decreasing the horizontal deviations between the two curves. The error that I found was that this reference center of the beam was being calculated incorrectly. As seen in figure 20, the upper left plot is the input distribution (i.e measured emittance data at XEMIT8 location) and the upper right plot is what the optimizer thinks the beam will look like with the multipole correction. The vertical blue line represents what the code calculates the reference center of the beam to be. The black curve represents the calculated centroid values that the optimizer will try to bring towards the blue line. Clearly, the calculated reference center of the beam is completely wrong. This is because it is mistakenly calculating the center of data that has been transposed for plotting purposes. The simple fix is making sure it is calculating the center of data that has not been transposed as seen in the lower two plots of figure 20. This has a relatively significant effect on the multipole configuration as with the incorrect reference beam center, the configuration is optimized to correct for aberrations AND *shift* the whole beam to be centered around the calculated reference center. This effect is seen in the upper right plot in figure 20.
Fixing these two errors has greatly improved the predicted configuration for some cases. However, there are still two more observed issues that require work. The first is more so a general characteristic of the system that has to be kept in mind and eventually worked into the code. For a 5k or 10k RP tune, the beam does not (relatively) get very large at the multipole location. But, recall from the multipole drawing (fig:13), that the HRS multipole is shaped like a large rectangle. This can be a problem as all the optimizer cares about currently is minimizing horizontal deviation from the reference center. In other words, it doesn't mind applying a large voltage to the edge poles even when this effect will be very small on a beam that is small at the multipole location. For a larger RP tune, the beam is larger at the multipole location and thus the poles will put a smaller potential on the edge poles to have an effect on the beam (i.e beam closer to edge poles). This will be more clear shortly via some simulations I run through the optmizer with ZGOUBI.
To summarize, if the beam is relatively small at the multipole location, the optimizer might put large potentials on the edge poles to have an effect on the beam. A fix to this could be as simple as an if statement that doesn't let the optimizer accept a configuration if it notices one of the poles is at a value larger than say 50V (brainstorm more on this).
The second issue I believe is related to the first and might be fixed alongside the first issue being fixed. However, it is fundamentally more complicated as it has to do with how the algorithm is built rather than just a geometry issue like the last one.

Since the system is over-determined, the method of least squares is applied to several different possible sets of equations. Following the algorithm, it calculates the total horizontal deviation at the end of each calculation for the different sets of equations. Then, the best set of equations to use and thus the best multipole configuration to use is simply determined by which ever set returns the smallest total horizontal deviation. The issue is then that sometimes the configuration with massive values on the poles is the set of equations that returns the smallest horizontal deviation. This can be seen in `Optimize.py` within the function `OptimizeLA`. The function loops over parameter `NoS` from 0 to 4 which defines the number of theta values/equations to skip between each theta value/equation that the optimizer decides to use. Within this loop, there is another loop over parameter `start` from 0 to 4 that simply affects the number of equations to skip before selecting the first one to use.
As an example, for the XEMIT8 data shown in figure 20, the optimizer chooses a configuration that yields a total horizontal deviation from the desired position of 0.05mm. The plot looks nicely corrected but the predicted configuration is highly questionable (see column A in table 3). A different set of equations, defined by $NoS = 3$, $start = 1$, yield a total horizontal deviation of 0.26mm. Despite the slightly larger horizontal deviation, the configuration calculated in this case seems much more reasonable (see column B in table 3). The current optimizer will not choose this 'more reasonable' configuration since the total horizontal deviation is larger. Furthermore, as seen in figure 21, there is no obvious difference between the expected emittance measurements despite the calculated multipole configurations being very different. This puts even more confidence in configuration B) being sufficient to correct aberrations for this emitttance measurement. Note that unfortunately these configurations were not tested with real measurements as this analysis and simulation work was done months after the measurement was taken and after the source had been switched from Potassium to Rubidium.

Another round of simulations I did involved testing simulated ZGOUBI distributions in the multipole configuration optimizer. Then, since the ZGOUBI model was found to agree with measurements (i.e fig:18), I could test the predicted multipole configuration in ZGOUBI to see if the aberrations are corrected. Additionally, this helps validate the mapping from ZGOUBI pole orientation to EPICS orientation (other than perhaps the edge poles since no measurements with them have been taken yet).
The first step for this involves binning the distributions in ZGOUBI to get x, y, z formatted data (see fig:22). In this simulation, I scaled the input distribution to have a larger angle range ($\pm 60\, mrad$) in order to test if the optimizer puts smaller potentials on the edge poles. The optimized configuration seems very reasonable as seen in column C) in table 3. This configuration yields a total horizontal deviation of 0.096mm and is purely the configuration the optimizer gives without having to artificially choose which `NoS` and `start` parameters to use. This simulation seems to indicate that the optimizer works better with data that has a larger angle range as then it will not put a large potential on edge poles that are very far from the beam. The next step is to use the multipole configuration as input in `Multipole.py`. The idea is that if this configuration corrects the aberrations then we can be relatively

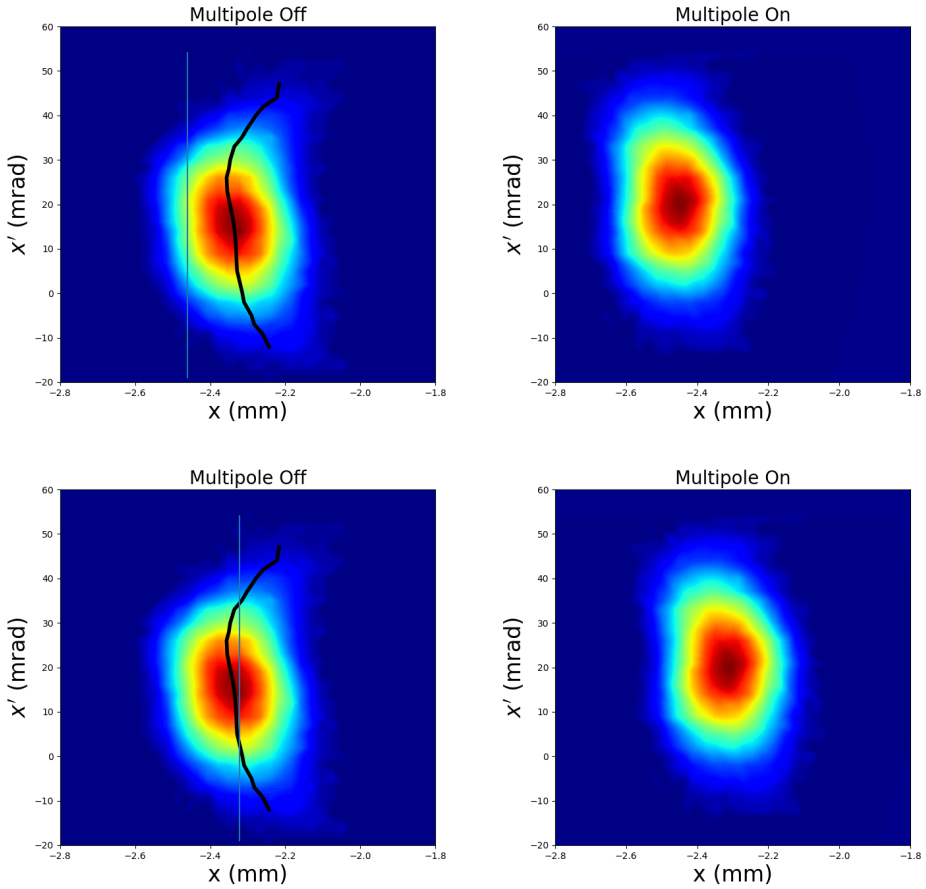

Figure 20: The left column shows the measurement data at XEMIT8 taken with the multipole off. This data is given to the multipole configuration optimizer as input. The blue line is the calculated reference center of the beam and the black line is the calculated centroid in position at each angle. The rightmost plots are what the optimizing code predicts the beam will look like when the multipole is set to a certain configuration (i.e these are not measurements). The top row is the original code that was calculating the reference center incorrectly and thus shifting the final beam position. The bottom row is when the reference center is being calculated correctly.

Electrode Pair Labels/Indices			Potential (V)		
HLA	EPICS	ZGOUBI	**A)**	**B)**	**C)**
20	2S	0	-1000.00	-0.08	-2.05
10	1S/3S	1	972.29	-0.10	0.93
01	19T/B	2	638.75	-0.12	-2.26
02	18T/B	3	-239.87	-0.36	-0.51
03	17T/B	4	-10.00	-0.83	-0.51
04	16T/B	5	4.18	-1.08	-0.26
05	15T/B	6	1.34	0.55	0.00
06	14T/B	7	1.82	0.53	0.14
07	13T/B	8	1.41	0.06	0.17
08	12T/B	9	1.09	-0.18	0.17
09	11T/B	10	1.67	0.08	0.04
0A	10T/B	11	1.21	-0.21	-0.07
0B	9T/B	12	2.02	-0.40	-0.18
0C	8T/B	13	0.73	0.60	-0.33
0D	7T/B	14	-12.13	0.84	-0.37
0E	6T/B	15	333.39	0.46	-0.37
0F	5T/B	16	-778.28	0.20	-0.09
0G	4T/B	17	927.01	0.08	0.65
0H	3T/B	18	-1000.00	0.04	1.52
0I	2T/B	19	-1000.00	0.01	2.21
0J	1T/B	20	-1000.00	0.00	4.09
1K	1N/3N	21	-1000.00	0.00	4.25
2K	2N	22	-1000.00	0.00	3.57

Table 3: The first three columns show the respective electrode pair index matching between the current HLA, EPICS and python/ZGOUBI. NOTE: this mapping is not 100% confirmed as we have not yet taken measurements with individually turning on the edge poles (i.e could be that the S and N poles in EPICS are swapped in this map for example). The map from HLA to python is confirmed to be accurate as this is simply comparing simulations to simulations.
The next three columns show different multipole configurations calculated by the optimizer. Column **A)** is the configuration for the emittance data shown in figure 20. The equations used correspond to $NoS = 0$, $start = 0$ and give a total horizontal deviation of $0.05mm$. The configuration is very bad in terms of putting unnecessarily large values on many of the edge poles. Column **B)** is a different configuration for the emittance data shown in figure 20. The equations used correspond to $NoS = 3$, $start = 1$ and give a total horizontal deviation of $0.26mm$. The optimizer disregards this configuration since the calculated horizontal deviation is larger. But, the configuration seems much more reasonable when considering the effects an individual pole at 5V has on the beam in measurements.
Column **C)** is the configuration for figure 22 data. The configuration seems reasonable considering the larger angle range in the simulated ZGOUBI data.

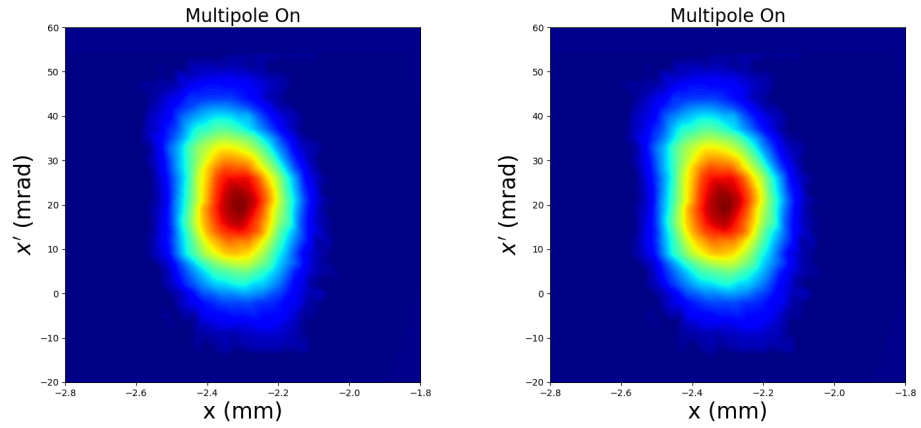

Figure 21: On the left is the simulated expected horizontal phase space measurement for the multipole configuration **A)** from table 3. On the right is the simulated expected horizontal phase space measurement for the multipole configuration **B)** from table 3. Despite the configurations being very different and the calculated total horizontal deviation being different, there is no significant differences in the two plots.

confident that the optimizer will calculate an accurate configuration for measurements since it's been shown that the ZGOUBI simulations with individual poles turned on match measurements. Figure 23 shows ZGOUBI simulations through the HRS when the multipole is turned on at the configuration calculated by the optimizing code. The aberrations appear to be adequately corrected in this simulation. The obvious next step is to take XEMIT8 measurements with aberrations in the beam and turn the multipole on to the optimized configuration and see if the aberrations are corrected. As of early August, the XEMIT8 measurements for 10k RP tune are shown in figure 6. Notably, there are no aberrations. I ran this measurement through the configuration optimizer and, as expected, the configuration had almost every single pole on 0V (max value on a pole was 0.22V). However, note that in order to get the code to run, I had to artificially bring down the angle to be less than 78 mrad. This is because the original design of the code only understands angles between -78 and 78 mrad and the measurement range was about 12 mrad to 105 mrad. Likely, a combination of trying to center the beam in angle more and improving the code to understand a wider angle range will correct this issue.

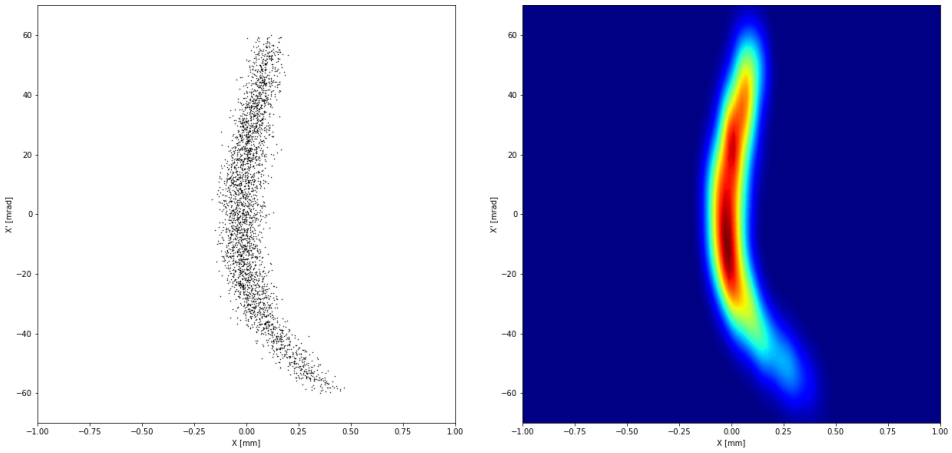

Figure 22: ZGOUBI simulations through the HRS with multipole off. These plots just show the scatter distribution (left) versus binning the data (right) for input into the multipole configuration optimizer. The input distribution was scaled to have a larger angle range via the scaling parameters in the 'OBJET' element: `(1. 1. 2. 0.25 1. 1.)`. This will test if the optimizer puts smaller values on the edge poles since the beam is bigger in position at the multipole location. The simulations here also have 2eV of energy spread.

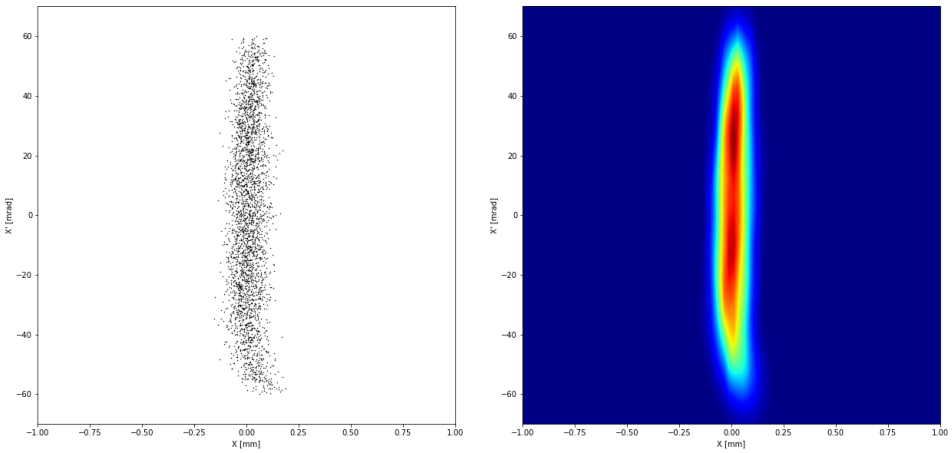

Figure 23: ZGOUBI simulations through the HRS with the multipole on at the configuration shown in column C) in table 3. The aberrations seem well corrected when compared to figure 22 where the multipole is off.

6 Summary

Overall, the functionality of the optical and (currently controllable) diagnostic elements in the CANREB HRS system have been verified for 5k and 10k RP. However, the matter of emittance growth through the HRS is still under investigation, with energy spread being the suspected cause. The HRS multipole has been tested and shown to function as intended, although additional measurements are required to prove the configuration optimizer works. In broad terms, future work includes: 1) Solving the emittance growth issue, 2) Taking vertical emittance measurements, 3) Testing multipole configurations for the purpose of correcting aberrations, 4) Degauss and ramp dipoles to optimize field flatness, and 5) Go to higher RP (15k and 20k).

References

[1] J. A. Maloney, M. Marchetto, R. Baartman, ARIEL High Resolution Separator, Tech. Rep. TRI-DN-14-06, TRIUMF (2014).

[2] S. Saminathan, M. Marchetto, CANREB HRS Commissioning Plan, Tech. Rep. Document-161577, TRIUMF (2019).

[3] R. Baartman, HRS Match/Magnifier Section, TRI-BN-18-12, TRIUMF (2018).

[4] S. Kiy, HRS Ramping Procedure, Tech. rep., TRIUMF (2019).

[5] Y.-N. Rao, Maximum Entropy Tomography Validation, Tech. Rep. TRI-BN-18-16, TRIUMF (2018).

[6] S. Saminathan, F. Ames, R. Baartman, M. Marchetto, O. Lailey, A. Mahon, Tomography reconstruction of beams extracted from an ion source, Review of Scientific Instruments 90 (12) (2019) 123302. doi:10.1063/1.5129786.
URL https://doi.org/10.1063/1.5129786

[7] O. Shelbaya, Maximum Entropy Tomography at the ISAC-RFQ, Tech. Rep. TRI-BN-20-12, TRIUMF (2020).

[8] Y.-N. Rao, Beam Tomography and Emittance Measurements in ISIS, Tech. Rep. TRI-BN-20-17, TRIUMF (2020).

[9] O. Lailey, Tomography Reconstruction for ARIEL CANREB Beam Commissioning, Tech. Rep. TRI-BN-19-07, TRIUMF (2019).

[10] A. Mahon, S. Saminathan, Preliminary CANREB Beamline Comissioning Results, Tech. Rep. TRI-BN-19-19, TRIUMF (2019).

[11] J. d. Luna, Phase Space Tomography at TRIUMF, Tech. Rep. TRI-BN-19-23, TRIUMF (2019).

[12] M. Bleszynski, ARIEL Basement-2 Level Beamline Commissioning Results, Tech. Rep. TRI-BN-19-24, TRIUMF (2019).

[13] L. Jensen, Tomography Simulation for the Profile Monitor in the ARIEL RIB Module, Tech. Rep. TRI-BN-20-02, TRIUMF (2020).

[14] J. A. Maloney, CANREB HRS Multipole Corrector, Tech. Rep. TRI-DN-16-09, TRIUMF (2016).

[15] T. Planche, TRIUMF High Resolution Separator using ZGOUBI, Tech. Rep. TRI-BN-17-19, TRIUMF (2017).

[16] D. Sehayek, Automatic Tuning Algorithm for the CANREB HRS Multipole, Tech. Rep. TRI-BN-17-17, TRIUMF (2017).

[17] D. Sehayek, R. Baartman, C. Barquest, J. Maloney, M. Marchetto, T. Planche, Multipole Tuning Algorithm for the CANREB HRS at TRIUMF, in: Proc. 9th International Particle Accelerator Conference (IPAC'18), Vancouver, BC, Canada, April 29-May 4, 2018, no. 9 in International Particle Accelerator Conference, JACoW Publishing, Geneva, Switzerland, 2018, pp. 4836–4838. doi:doi:10.18429/JACoW-IPAC2018-THPML079.